J Mater Sci (2011) 46:7437–7442
DOI 10.1007/s10853-011-5708-0

Study of intrinsic white light emission and its components from ZnO-nanorods/*p*-polymer hybrid junctions grown on glass substrates

I. Hussain · N. Bano · S. Hussain · O. Nur · M. Willander

Received: 10 February 2011 / Accepted: 10 June 2011 / Published online: 21 June 2011

Abstract We report white-light luminescence from ZnO-organic hybrid light emitting diodes grown on glass substrate by low temperature aqueous chemical growth. The configuration used for the hybrid white light emitting diodes (HWLEDs) consists of two-layers of polymers (PEDOT:PSS/PFO) on glass with top ZnO nanorods. Electroluminescence spectra of the HWLEDs demonstrate the combination of emission bands arising from the radiative recombination in polymer and ZnO nanorods. In order to distinguish emission bands we used a Gaussian function to simulate the experimental data. The emitted white light was found to be the superposition of a blue line at 454 nm, a green emission at 540 nm, orange line at 617 nm, and finally a red emission at 680 nm. The transitions causing these emissions are identified and discussed in terms of the energy band diagram of the hybrid junction. Color coordinates measurement of the WLED reveals that the emitted light has a white impression with 70 color rendering index and correlated color temperature 5500 K. Comparison between ITO and aluminum top contacts and its influence on the emitted intensity is also discussed.

Introduction

Zinc oxide (ZnO) with wurtzite structure has emerged to become one of the prime materials for photonics applications with potential advantages over the III-nitride system due to the high exciton binding energy 60 meV (GaN has 25 meV) [1]. Such a relatively high value of the exciton binding energy would imply that ZnO will have stable excitonic emission even above room temperature. Beside the potential for developing optoelectronic devices, ZnO is biocompatible and bio-safe material, owing to these properties ZnO is considered as an important environment friendly wide bandgap semiconductor material [2–4]. ZnO has attracted a renewed global interest due to the fact that it also possesses a rich family of nanostructures which can be grown on alien substrates without the need of lattice matching [1]. The growth of ZnO nanostructures can be achieved using different high as well as low temperature (<100 °C) growth approaches [4]. The most usual high-temperature techniques used are metal-organic chemical vapor deposition (MOCVD) [1] and vapor liquid solid (VLS) [1], these methods require expensive equipment and need to done in extreme conditions. Therefore, low temperature and cost techniques which are restricted to aqueous chemical growth (ACG) process are preferred. In addition to the above mentioned properties ZnO possesses a large number of radiative intrinsic and extrinsic deep level defects [5–7]. Specifically ZnO, beside the ultraviolet (UV) emission due to band gap, emits blue, green, yellow, and orange-red colors; which covers the whole visible region [5–8]. Therefore, the optical properties of ZnO have been extensively studied and at room temperature. ZnO typically exhibits one sharp UV peak and possibly one or two deep level emissions (DLE) due to deep defect states in the bandgap [7, 8]. The dominant emitted colors depend on the growth methods and its parameters and this implies that the emitted color lines can be controlled [6]. Hence ZnO is of great potential to the development of white light emitting diodes (WLEDs).

Recently, the application of ZnO in efficient solid-state lighting becomes the subject of several studies [9]. However, the stable and reproducible p-type doping in ZnO is still a

I. Hussain (✉) · N. Bano · S. Hussain · O. Nur · M. Willander
Department of Science and Technology, Campus Norrköping, Linköping University, 60174 Norrköping, Sweden
e-mail: ijaas@ifm.liu.se; ijaz75@hotmail.com

problem which is hindering the realization of a ZnO p–n homojunction diodes [1]. However, growing ZnO nanostructures on other inorganic/organic p-type substrates could provide an alternative way to realize ZnO-based p–n heterojunctions. In recent years ZnO-organic HWLEDs is one of the most exciting research areas. It has been reported that inorganic and organic materials could form a complex device to realize emissions from both kinds of materials [10]. Many researchers have prepared LEDs based on nano structured ZnO and p-type polymers such as poly(3,4-ethylenedioxythiophene) poly(styrenesulfonate) (PEDOT:PSS) [11, 12] and *N,N*′di(naphtha-2-yl)-*N,N*′-diphenyl-benzidine (NPB) [9]. *N,N*′-diphenyl-*N,N*′-bis(3-methylphenyl)-(1,1′-biphenyl)-4,4′-diamine (TPD), poly(9-vinylcarbazole) (PVK), 4,4′-bis(*N*-carbazolyl)-1,1′-biphenyl (CBP) [13]. However, efficient intense white-light luminescence from ZnO-organic hybrid LEDs has remained an enduring challenge. We have previously demonstrated multilayer and blended polymers which have high turn on voltage (14 V) and blue dominated broad band emission [14]. Now the configuration used for HWLEDs consists of two-layers of polymers on glass with top ZnO nanorods grown by the aqueous chemical growth (ACG). An inorganic/organic heterojunction has been fabricated by spin coating the p-type polymer poly(3,4-ethylenedioxythiophene) poly (styrenesulfonate) (PEDOT:PSS) for hole injection with an ionization potential of 5.1 eV and Poly(9,9-dioctylfluorene) (PFO) is used as blue emitting material with a bandgap of 3.3 eV and high occupied molecular orbital (HOMO) of 5.8 eV [15, 16]. On top of the polymers, ZnO nanorods were grown which are used as an electron transporting and emitting layer. The chemical structures of polymers used in this study can be found in [16, 17]. The transparent conducting indium tin oxide (ITO) is used to get the improved light output intensity.

In this article we report intrinsic white-light luminescence from ZnO-organic HWLEDs grown on glass substrate by low temperature aqueous chemical technique. Electrically driven ZnO-organic HWLEDs were constructed as well as its electrical and optical properties were measured and analyzed using different techniques, including scanning electron microscope (SEM), current–voltage (*I–V*), room temperature (RT) photoluminescence (PL), and RT electroluminescence (EL) measurements. The RT-EL spectrum demonstrates the combination of broad emission bands emerging from the radiative recom bination in polymer and ZnO nanorods. In order to distinguish the white-light EL spectrum components and the contribution of the PFO polymer layer we used a Gaussian function to simulate the experimental data. The transitions causing these emissions are identified and discussed in terms of the energy band diagram of the hybrid junction.

Experimental details

To fabricate ZnO-organic HWLEDs on glass substrate, first the glass was washed in ultrasonic cleaner in isopropyl alcohol, acetone, and de-ionised water sequentially. PEDOT:PSS was then spin-coated onto the treated glass and baked at 150 °C to form a uniform film. We cover small portion of PEDOT:PSS for ohmic contact and PFO was spin coated on top of the PEDOT:PSS film and backed at 100 °C for 5 min. To improve the ZnO nanorods growth quality, distribution, and density a seed layer is spin-coated three time and baked for 3 min at 100 °C [18]. To grow ZnO nanorods we use a low temperature chemical growth technique. In this method 0.01 M zinc nitrate hexa hydrate ($Zn(NO_3)\cdot 6H_2O$) were mixed with 0.01 M Hexamethyl tetra-mine (HMT) ($C_6H_{12}N_4$). The sample was placed in the solution and was heated at 96 °C for 4 h. After that it was washed with deionized water. After growth, the samples were used to process light emitting diodes (LEDs). Silver paste is used for the ohmic contact on PEDOT:PSS. Prior to the ohmic contacts on the ZnO NRs, an insulating PMMA layer was deposited between the NRs. Recently it was shown that the use of PMMA as an insulating layer between nanorods will lead to enhance the emission intensity due to the change of surface states [19]. To insure that no PMMA was on the top of the NRs, oxygen plasma cleaning was performed prior to the contact metal deposition. Then on one sample the indium tin oxide (ITO) circular transparent contacts of 1.2 mm in diameter and thickness of 700 Å were evaporated onto a group of NRs and on other sample the Al circular contacts of 1.2 mm in diameter and thickness of 700 Å were evaporated onto a group of NRs. A schematic diagram of the device is shown in Fig. 1. The device structure was characterized by a scanning electron microscope, X-ray diffraction, and photoluminescence at room temperature. The RT-EL measurement of the ZnO-organic HWLEDs was carried out using a photo multiplier detector under dc-bias condition. The light was collected from the topside of the device.

Results and discussion

The ZnO NRs grown on multi-layer polymer were found to be aligned vertically and distributed uniformly as shown in the SEM image in Fig. 2. The inset shows the SEM image after spin coating insulating layer and followed by soft backing.

Figure 3 exhibits the RT-PL spectra of PFO and HWLEDs. The RT-PL spectrum of PFO (without ZnO NRs) reveals two violet emissions at 429 and 451 nm, and one broad blue–green emission centered at 482 nm. The RT-PL spectra HWLEDs consisted of UV emission

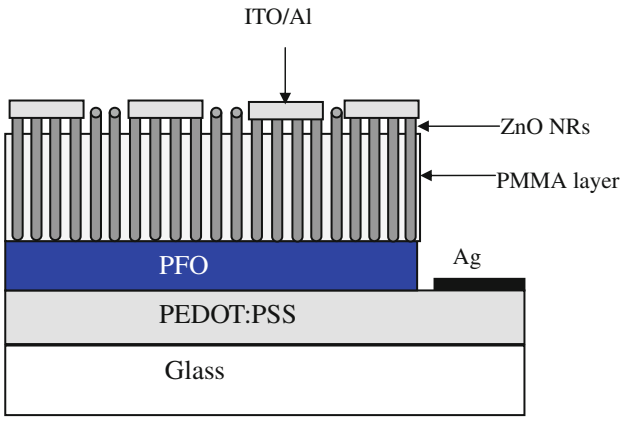

Fig. 1 Schematic illustration of ZnO NRs/PFO/PEDOT:PSS heterostructure device

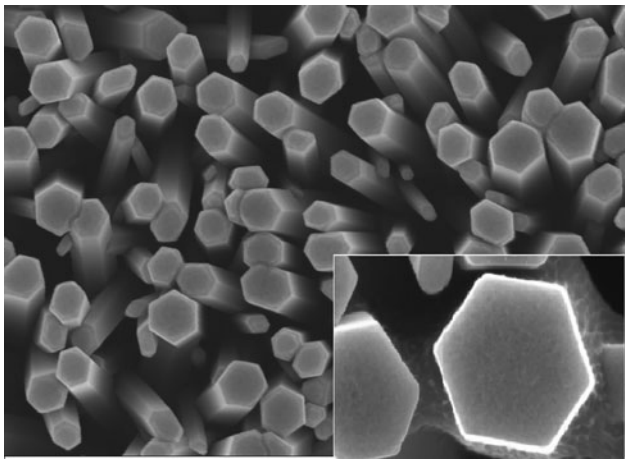

Fig. 2 SEM image of as grown ZnO NRs on PFO polymer and *inset* shows the SEM image after spin coating and followed by soft baking

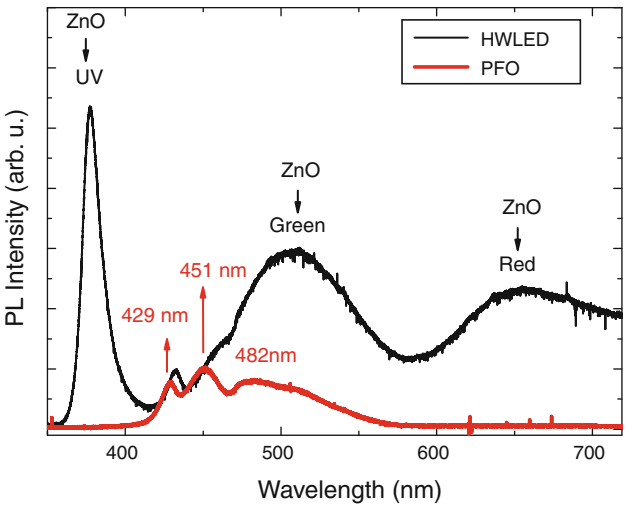

Fig. 3 Room temperature PL spectrum of the ZnO NRs/PFO hybrid structure and the PL spectrum of the PFO on glass substrate

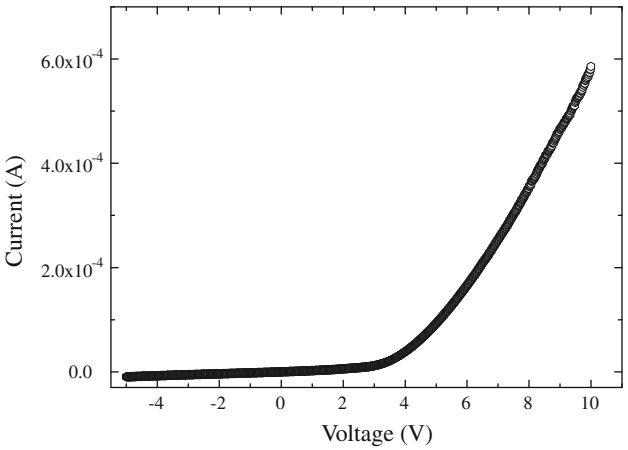

Fig. 4 Typical room temperature *I–V* characteristics of ZnO NRs/PFO/PEDOT:PSS heterojunction

centered at around 380 nm, PFO violet-blue emission at 432–450 nm and two DLE bands from ZnO NRs green at 512 nm and red at 652 nm. It is extensively reported that the DLE is a superposition of many different deep levels emitting at the same time [7]. The origin of the DLE has been controversial for decades. This is probably one reason for the debate, since different samples have different defect configuration due to the different growth methods and growth conditions. The peak position of the deep band emission is defined according to the relative density of these radiative defects. The probable intrinsic deep level defects in ZnO are oxygen vacancy (V_O), zinc vacancy (V_{Zn}), oxygen interstitial (O_i), zinc interstitial (Zn_i), oxygen anti-site (O_{Zn}), and zinc anti-site (Zn_O). These deep level defects often control directly or indirectly the luminescence efficiency in semiconductors [20].

Figure 4 shows the current–voltage (*I–V*) characteristics of the heterojunction. The diode-like behavior of heterojunction was examined using the thermionic emission model. According to this theory, the current in such a device could be expressed as

$$I = I_s\left[\exp\left(\frac{q(V - IR_s)}{nkT}\right) - 1\right] \quad (1)$$

where I_s is the saturation current, R_s is the series resistance, k is the Boltzmann constant, T is the absolute temperature, q is the elementary electric charge, V is the applied voltage, and n is the ideality factor. The ideality factor from Eq. 1 was found to be in the range 2.8–4 for all diodes investigated. The value of the ideality factor is comparable to the recently reported value of ideality factor for polymer heterojunction [4]. The higher value of ideality factor indicates that the behavior of heterojunction diode deviates from the ideal thermionic behavior. This may be due to the presence of surface states in ZnO. These surface states provide additional energy states which are responsible for

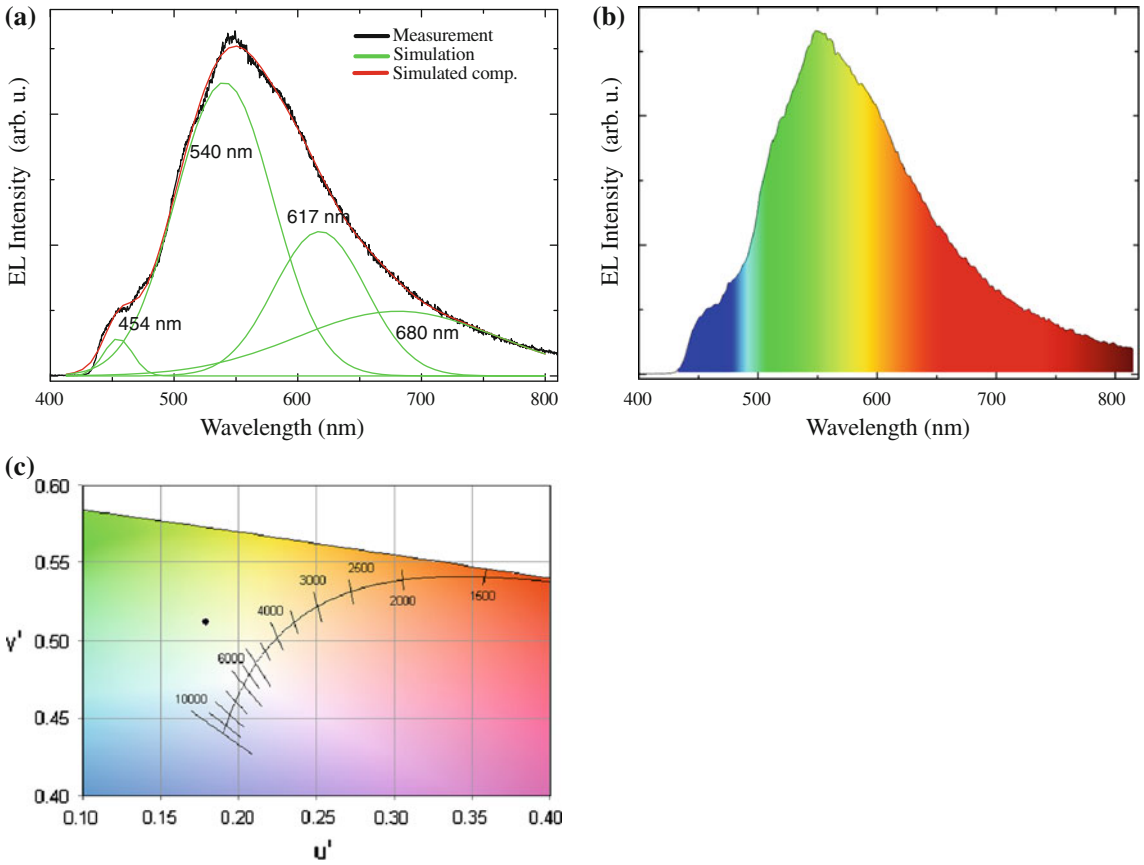

Fig. 5 **a** Room temperature EL spectrum after a Gaussian fitting. **b** The EL spectrum showing the whole visible range which is distinguished by a Gaussian fitting. **c** The Chromaticity diagram of the HWLED

the existence of multiple current pathways [4]. In our case, a lot of defects have been verified by defect related PL bands in ZnO NRs and PFO, which provide additional energy states and hence multiple current pathways.

The RT-EL spectra of HWLEDs reveal a broad emission band from 420 to 800 nm covering the whole visible region as shown in Fig. 5a. In order to distinguish the white-light EL spectra components we used a Gaussian function to simulate experimental data. The simulated EL spectrum shows four emissions at 454, 540, 617, and 680 nm which are associated with blue, green, orange, and red, respectively. It is clear that the emission at 454 nm (blue) is due to the radiative recombination in PFO and green–red (540–680) emissions are associated with radiative defects in ZnO. The green luminescence band is the most investigated and most debated band in ZnO. The variation in the green emission peak position is attributed to different relative contributions from, e.g., V_O, V_{Zn}, Zn_i, O_i, and Cu related defects caused by fluctuations in the growth conditions for different growth methods [21]. Recently, the green emission has been explained to be originating from more than one deep level defect, V_O and V_{Zn} with different optical characteristics were found to contribute to the broad green luminescence band [8, 21]. Moreover, the orange emission was recently attributed to oxygen interstitial, while the red emission was attributed to the transition associated to zinc interstitials [22]. However, no consensus has been reached regarding the origin of the different observed colors, partly due to the different defect configuration in different samples [6, 23]. The Fig. 5b demonstrates the RT-EL spectra with all emissions which are distinguished by a Gaussian function. To investigate color quality of LEDs color chromaticity coordinates are plotted in Fig. 5c. Figure 5c shows the emitted light has a white impression. The color rendering index (CRI) and correlated color temperature (CCT) of the LEDs were calculated to be 70 and 5500 K, respectively.

Room temperature EL and PL spectra of HWLEDs with PL spectra of PFO (without ZnO) are shown in Fig. 6. Figure 6 obviously demonstrates that the EL bands of the HWLEDs are consistent with the sum of the PL bands of individual PFO and ZnO components. It is essential to mention that the PFO blue peaks are completely intermixed with the DLE bands of the ZnO NRs resulting in the single broad band. But the UV emission of the ZnO NRs is not detected in the EL spectra probably due to the self-absorption of the UV light by the ZnO direct bandgap and/

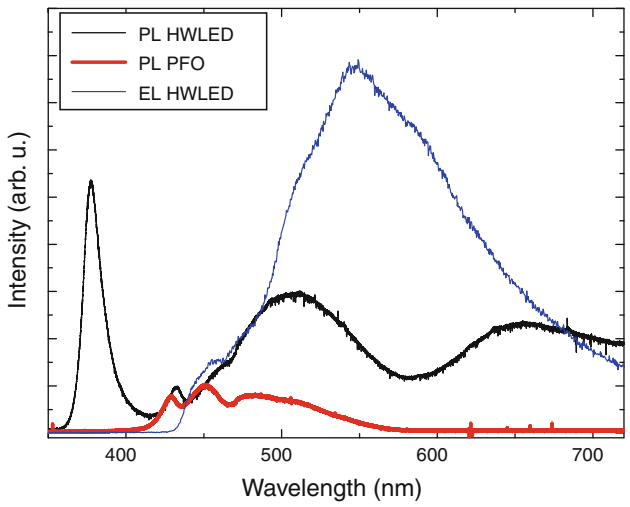

Fig. 6 Room temperature EL and PL spectra of HWLEDs with PL spectra of PFO (without ZnO)

or absorption by the PFO at the ZnO/PFO interface [19]. Do-Hoon Hwang et al. [24] reported that polyfluorenes (PFs) exhibit absorption maxima close to 380 nm. The concentration of PFO polymer has vital role on optical efficiency and light quality of the HWLEDs.

Now we discuss the EL emission of the WLEDs by using the energy band diagram. The energy band diagrams of the WLEDs without and with bias voltage are shown in Fig. 7a, b. It can be seen in Fig. 7a that there is a 0.9 eV barrier for hole injection from Ag to the PEDOT:PSS HOMO (highest occupied molecular orbit), 0.6 eV barrier from the PEDOT:PSS to the PFO HOMO and there is a 2 eV barrier for hole injection from the PFO HOMO to the ZnO valence band. The electron injection barrier is 0.5 eV between the ITO Fermi level and the ZnO conduction band, and 1.7 eV barrier for electron injection from the ZnO conduction band to the PFO LUMO (lowest unoccupied molecular orbit). When the device is biased the barriers normally cause hole and electron accumulation and energy band bending at the organic/ZnO interface [9]. The electrons and the holes under forward bias accumulate at the ZnO NRs/PFO interface, as shown in Fig. 7b. The white-light EL might be attributed to the excitonic emissions resulting from the recombination of the electrons and the holes at ZnO NRs/PFO interface. The lifetime of the electrons existing in the ZnO/PFO interface is much larger than that in the ZnO NRs [25]. The electrons existing at the interface between the conduction band edge of the ZnO NRs and the LUMO level of the PFO layer slowly drop to the lower states because of their longer life time. Therefore, the emission with various wavelengths is emitted due to continuous recombination between the electrons and the holes during electron transitions from the upper states to the lower states [25]. We have many radiative defects in ZnO NRs and in the bulk of PFO polymer. The energy states of various native radiative defects had been calculated or experimentally measured in the band gap of ZnO. The commonly observed green emission is frequently attributed to transition from conduction band to V_O. Moreover, the orange emission was recently attributed to transition from the conduction band to O_i, while the red emission was proposed to be due from transition Zn_i to O_i [6]. Lee et al. [26] reported the EL emission at 454 nm (blue) that is due to the exciton emission in the PFO. This PFO related blue emission combined with ZnO defect related emissions results in the intrinsic white-light emission. But the brightness and efficiency of the white light is dependent on the concentration/thickness of the polymers and transparent contact. Chang et al. [27] reported that the hole-injection barrier of PFO decreases and the brightness/efficiency of ZnO-organic HWLEDs increases with decreasing the PEDOT:PSS thickness. For the general admitted property of PFO bipolar devices, green light will emit at high voltage resulting from a formation of excimer, and this green light emission will give rise to higher brightness and efficiency [27]. So we used thin polymer layers and transparent ITO contact to increase the brightness of HWLEDs. The average optical transparency of ITO is 95% for the 400–800 nm wavelengths [28]. Figure 8 shows the

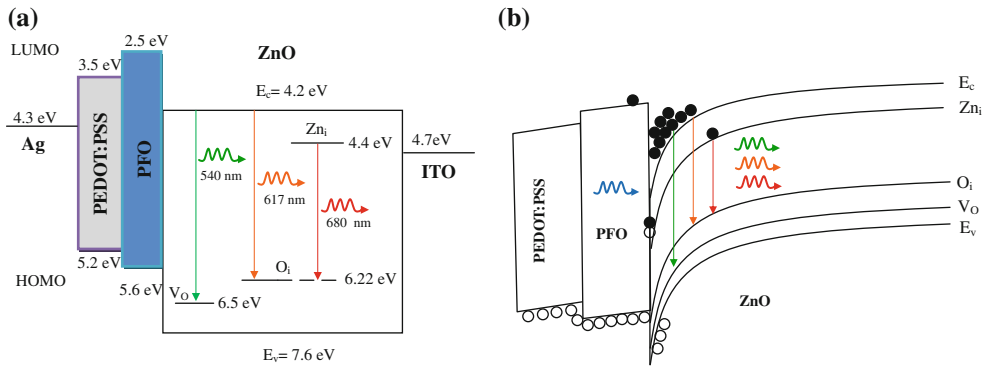

Fig. 7 **a** Energy band diagram of ZnO NRs/PFO hybrid heterojunction showing the EL emissions from ZnO NRs. **b** Energy band diagram of ZnO NRs/PFO hybrid heterojunction under forward bias showing band banding at the interface and charge accumulation

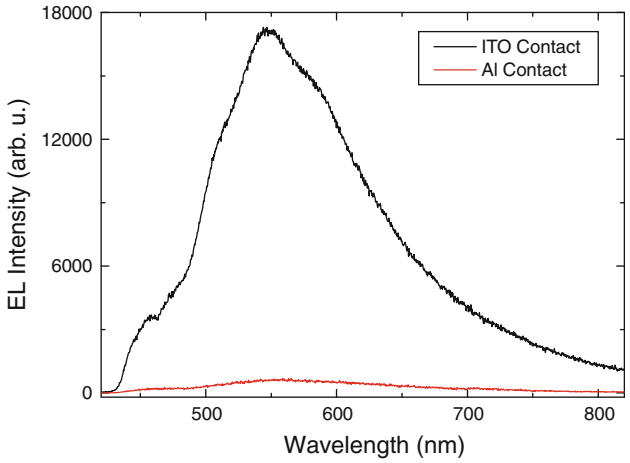

Fig. 8 The comparison of HWLEDs EL spectra with Al and ITO contacts at 2 mA current

comparison of EL spectra of HWLEDs with Al and ITO contacts at 2 mA current which demonstrates the intensity/brightness of white light can be increase 35 times by using transparent contact. The combination of transparency in the visible range, thin polymer layers and low temperature procedure makes the organic–inorganic hybrid junction WLEDs attractive for the development of large area lighting source compatible with existing armature technologies.

Conclusion

In conclusion, intrinsic white-light luminescence from ZnO-organic hybrid light emitting diodes grown on glass substrate by low temperature aqueous chemical growth (ACG) has been demonstrated. The configuration used for the hybrid white light emitting diodes (HWLEDs) consists of two-layers of polymers PEDOT:PSS and PFO on glass with top ZnO nanorods (NRs). The EL spectrum reveals a broad emission band covering the range from 420 to 800 nm emerging from the radiative recombination in polymer and ZnO nanorods. In order to distinguish the white-light components we used a Gaussian function to simulate the experimental data. The emitted intrinsic white light was found to be the superposition of a blue line at 454 nm from PFO and green emission at 540 nm, red emission at (617–680 nm) are due to radiative defect emissions in ZnO nanorods. The transitions causing these emissions are identified and discussed in terms of the energy band diagram of the hybrid junction. The intensity/brightness of HWLEDs is increased by using transparent ITO contact with high optical transparency in visible range. The combination of transparency in the visible range and low temperature procedure makes the organic–inorganic hybrid junction WLEDs attractive for the development of low cost and large area lighting sources.

References

1. Willander M, Nur O, Zhao QX, Yang LL, Lorenz M, Cao BQ, Zúñiga Pérez J, Czekalla C, Zimmermann G, Grundmann M, Bakin A, Behrends A, Al-Suleiman M, El-Shaer A, Che Mofor A, Postels B, Waag A, Boukos N, Travlos A, Kwack HS, Guinard J, Le Si Dang D (2009) Nanotechnology 20:332001
2. Cheng K, Cheng G, Wang S, Li L, Dai S, Zhang X, Zou B, Du Z (2007) New J Phys 9:214
3. Sadik PW, Pearton SJ, Norton DP, Lambers E, Ren F (2007) J Appl Phys 101:104514
4. Bano N, Zaman S, Zainelabdin A, Hussain S, Hussain I, Nur O, Willander M (2010) Appl Phys 108:043103
5. Willander M, Nur O, Bano N, Sultana K (2009) New J Phys 11:125020
6. Ahn CH, Kim YY, Kim DC, Mohanta SK, Cho HK (2009) J Appl Phys 105:013502
7. Bano N, Hussain I, Nur O, Willander M, Wahab Q, Henry A, Kwack HS, Le Si Dang D (2010) J Lumin 130:963
8. Børseth TM, Svensson BG, Kuznetsov AY, Klason P, Zhao QX, Willander M (2006) Appl Phys Lett 89:262112
9. Sun XW, Huang JZ, Wang JX, Xu Z (2008) Nano Lett 8:1219
10. Zhao S-L, Kan P-Z, Zheng X, Kong C, Wang D-W, Yan Y, Wang Y-S (2010) Org Electron 11(5):789
11. Könenkamp R, Word PC, Godinez M (2005) Nano Lett 5:2005
12. Chang CY, Tsao FC, Pan CJ, Chi GC, Wang HT, Chen JJ, Ren F, Norton DP, Pearton SJ, Chen KH, Chen LC (2006) Appl Phys Lett 88:173503
13. Liu J, Ahn YH, Park JY, Koh KH, Lee S (2009) Nanotechnology 20:445203
14. Wadeasa A, Beegum SL, Raja S, Nur O, Willander M (2009) Appl Phys A 95:807
15. Wan AS, Mäkinen AJ, Lane PA, Kushto GP (2007) Chem Phys Lett 446:317
16. Chen P, Yang G, Liu T, Li T, Wang M, Huang W (2006) Polym Int 55:473
17. Yu S, Ma C, Cheng C, Wang X, Ji D, Fan Z, Xia D, He W, Chang Y, Du G (2008) Dyes Pigm 76:492
18. Vafaee M, Youzbashizade H (2007) Mat Sci Forum 553:252
19. Liu KW, Chen R, Xing GZ, Wu T, Sun HD (2009) Appl Phys Lett 96:023111
20. Janotti A, Van de Walle CG (2009) Rep Prog Phys 72:126
21. Klason P, Børseth TM, Zhao QX, Svensson BG, Yu K, Willander M (2008) Solid State Commun 145:321
22. Djurisic AB, Leung YH, Tam KH, Hsu YF, Ding L, Ge WK, Zhong C, Wong KS, Chan WK, Tam HL, Cheah KW, Kwok WM, Phillips DL (2007) Nanotechnology 18:095702
23. Zainelabdin A, Zaman S, Amin G, Nur O, Willander M (2010) Nanoscale Res Lett 5:1442
24. Hwang D-H, Cho N, Jung B-J, Shim H-K, Lee J-I, Lee-Mi D, Zyung T (2002) Opt Mater 21:199
25. Son DI, You CH, Kim WT, Kim TW (2009) Nanotechnology 20:365206
26. Lee CY, Wang JY, Chou Y, Cheng CL, Chao CH, Shiu SC, Hung SC, Chao JJ, LiuM Y, Su WF, Chen YF, Lin CF (2009) Nanotechnology 20:425202
27. Chang C-H, Liao J-L, Hung M-C, Chen S-A (2007) Appl Phys Lett 90:063
28. Zhao J, Yang Z, Han S, Ye L, Xie S (2001) Displays 22:101